Molecular Cell, Vol. 15, 951–964, September 24, 2004, Copyright ©2004 by Cell Press

Structure and Stability of Cohesin's Smc1-Kleisin Interaction

Christian H. Haering,[1] Doris Schoffnegger,[1] Tatsuya Nishino,[1] Wolfgang Helmhart,[1] Kim Nasmyth,[1,*] and Jan Löwe[2,*]
[1]Research Institute of Molecular Pathology (IMP)
Dr. Bohr-Gasse 7
A-1030 Vienna
Austria
[2]MRC Laboratory of Molecular Biology
Hills Road
Cambridge CB2 2QH
United Kingdom

Summary

A multisubunit complex called cohesin forms a huge ring structure that mediates sister chromatid cohesion, possibly by entrapping sister DNAs following replication. Cohesin's kleisin subunit Scc1 completes the ring, connecting the ABC-like ATPase heads of a V-shaped Smc1/3 heterodimer. Proteolytic cleavage of Scc1 by separase triggers sister chromatid disjunction, presumably by breaking the Scc1 bridge. One half of the SMC-kleisin bridge is revealed here by a crystal structure of Smc1's ATPase complexed with Scc1's C-terminal domain. The latter forms a winged helix that binds a pair of β strands in Smc1's ATPase head. Mutation of conserved residues within the contact interface destroys Scc1's interaction with Smc1/3 heterodimers and eliminates cohesin function. Interaction of Scc1's N terminus with Smc3 depends on prior C terminus connection with Smc1. There is little or no turnover of Smc1-Scc1 interactions within cohesin complexes in vivo because expression of noncleavable Scc1 after DNA replication does not hinder anaphase.

Introduction

Sister chromatid cohesion is essential for bi-orientation of sister chromatids on the mitotic spindle. It is mediated by the multisubunit cohesin complex consisting of Smc1, Smc3, Scc1, and Scc3 proteins. The N- and C-terminal halves of Smc1 and Smc3, like other members of the structural maintenance of chromosomes (SMC) family, fold back on themselves to form 50 nm long intramolecular coiled coils. Their N- and C-terminal domains together form an ABC-like ATPase at one end (the "head") of the coiled coil while their central sequences form a dimerization or "hinge" domain at the other end, through which Smc1 and Smc3 interact to form a V-shaped heterodimer (Anderson et al., 2002; Haering et al., 2002; Melby et al., 1998). Crystal structures of the SMC-related Rad50 protein (Hopfner et al., 2000) and other ABC-like ATPases (Chen et al., 2003; Locher et al., 2002; Smith et al., 2002) suggest that ATP bound to each head induces their intimate interaction via contacts between ATP's phosphates and the adjacent head's signature motif residues. If this were also true for SMC proteins, then ATP would induce formation of a bipartite ring-like structure while its hydrolysis might drive heads apart, recreating V-shaped heterodimers. It is also conceivable that under special circumstances ATP could trigger interaction of heads from different SMC dimers (Hirano et al., 2001).

Cohesin's Scc1 subunit is a member of the kleisin superfamily of proteins, which are known to form complexes with SMC proteins (Schleiffer et al., 2003). Eukaryotic genomes encode at least three classes of kleisins: α kleisins like Scc1 and its meiotic counterpart Rec8, which interact with cohesin's Smc1/3 heterodimers, and β and γ kleisins, which interact with condensin's Smc2/4 heterodimers. The yeast Scc1 α kleisin is composed of three domains: an N-terminal region that interacts with Smc3's ATPase head, a C-terminal region that interacts with Smc1's ATPase head, and a central domain that contains cleavage sites for a thiol protease called separase (Uhlmann et al., 2000). Scc1 thereby forms a stable bridge connecting the two heads of Smc1/3 heterodimers to form a tripartite cohesin ring (Gruber et al., 2003; Haering et al., 2002). The connection between Smc1 and Smc3 heads provided by Scc1 is essential for sister chromatid cohesion. Thus, loss of cohesion at the metaphase-to-anaphase transition is triggered by proteolytic cleavage of Scc1's central domain by separase, which is activated through the destruction of an inhibitory chaperone (securin) by an ubiquitin protein ligase called the anaphase-promoting complex or cyclosome (APC/C). Scc1's cleavage at the metaphase-to-anaphase transition causes dissociation of cohesin from chromosomes with its N- and C-terminal cleavage fragments still bound to Smc3 and Smc1 heads, respectively. It is feasible that cohesin holds sister DNAs together by trapping them inside its tripartite ring structure and that separase destroys sister chromatid cohesion by opening the ring and thereby releasing previously entrapped DNAs.

The significance of ATP binding and hydrolysis by cohesin's SMC heads has been investigated by introducing mutations predicted to abolish either ATP binding, ATP-mediated dimerization via signature motifs, or hydrolysis of ATP bound to Smc1's or Smc3's head (Arumugam et al., 2003; Weitzer et al., 2003). Mutations to prevent binding of ATP to Smc1's head abolish association of Scc1 with Smc1/3 heterodimers in vivo. Equivalent mutations in Smc3 also inactivate cohesin but do not prevent Scc1 association. These experiments also suggest that binding of Scc1 to Smc1's head may be the first step in the formation of tripartite cohesin rings. Although mutant Smc1 or Smc3 proteins presumably defective in ATP hydrolysis form cohesin complexes, these complexes fail to associate stably with chromosomes. This raises the possibility that entry of DNA within cohesin's ring may depend on dissociation of Smc1 from Smc3 heads triggered by ATP hydrolysis.

To understand how Scc1 binds to Smc1's head, we have solved the crystal structure of a complex between Scc1's C-terminal domain and Smc1's ATPase head in

*Correspondence: knasmyth@imp.univie.ac.at (K.N.); jyl@mrc-lmb.cam.ac.uk (J.L.)

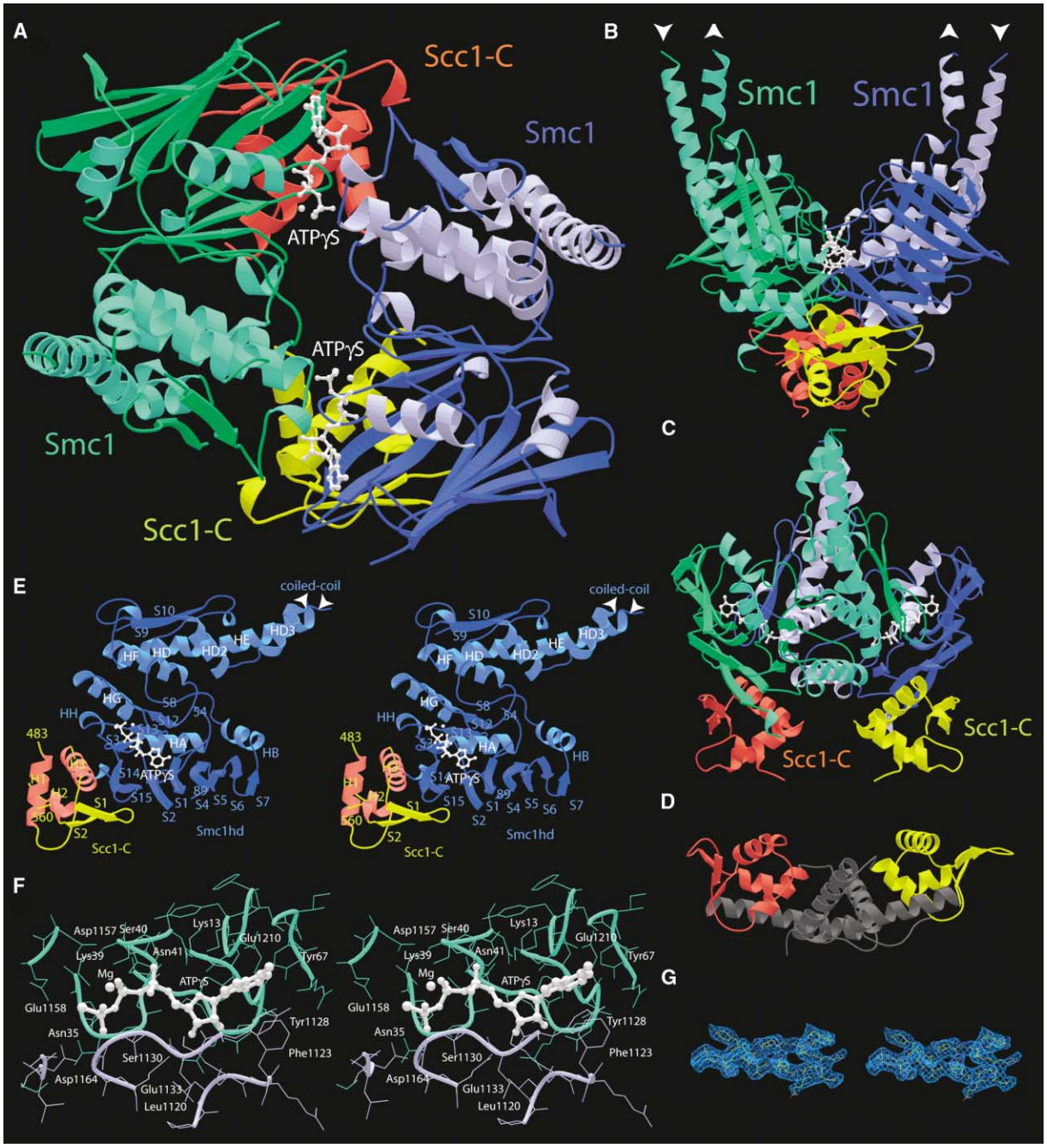

Figure 1. Structure of Smc1hd/Scc1-C

(A–C) Smc1hd/Scc1-C homodimer complexed with MgATPγS. The ABC signature motif comes close to the phosphates of the nucleotide. The C-terminal WHD of Scc1 binds to the side opposite of the coiled coil segments on Smc1.

(D) SarS (1P4X), the top score in a 3D similarity search to Scc1-C, encodes two WHDs by a single chain in approximately the same distance and orientation (rms 1.6 Å per domain, 3.6 Å overall). The DNA binding surface (top) of SarS corresponds to the Smc1 binding surface of Scc1-C.

(E) Stereo plot of Smc1hd/Scc1-C with assigned secondary structure elements.

(F) Detailed stereo plot of Smc1hd's ATP binding pocket.

(G) Final $2f_of_c$ electron density map of residues 1097–1116 of subunit chain C (Smc1).

the presence of ATPγS. The structure shows two dyad-related Smc1 heads each bound to Scc1 which sandwich a pair of ATPγS molecules in-between their contact surfaces. A similar structure possibly occurs between Smc1 and Smc3 heads in native cohesin complexes. Scc1 binds to the Smc1 head via a winged helix motif normally associated with DNA binding proteins. Mutation of specific Scc1 or Smc1 residues prevents complex formation between Scc1 and Smc1/3 heterodimers and abolishes cohesin function in vivo. By expressing sepa-

Table 1. Refinement Statistics, *S. cerevisiae* Smc1hd Domain/Scc1-C Terminus

Model	4-NCS-related Smc1hd:Scc1-C molecules in two dimers: Smc1 chain A, aa 2–52, 62–69, 89–169, 1067–1083, 1095–1100, 1113–1223 Smc1 chains B–D, aa 2–54, 62–69, 89–189, 1048–1083, 1095–1223 Scc1-C chains E–H, aa 483–512, 521–560 4 ATPγS, 4 Mg^{2+} 0 water molecules
Diff. data	NATI, 2.9 Å, all data
R factor, R free[a]	0.242 (0.397), 0.275 (0.394)
B factors[b]	66 $Å^2$, 3.1 $Å^2$
Geometry[c]	0.008Å, 1.456°
Ramachandran[d]	86.7%/0.1% (2)
Restrained NCS	
Smc1hd	0.197 Å
Scc1-C	0.120 Å
PDB ID	1W1W

[a] 5% of reflections were randomly selected for Rfree. R factors for the highest resolution bins are given in brackets.
[b] Temperature factors averaged for all atoms and rms deviation of temperature factors between bonded atoms.
[c] Rms deviations from ideal geometry for bond lengths and restraint angles.
[d] Percentage of residues in the "most favored region" of the Ramachandran plot and percentage of outliers, corresponding number of residues in brackets.

rase-uncleavable Scc1 variants in postreplicative cells, we find little or no exchange of cohesin or its subunits in vivo.

Results and Discussion

Structure of the Smc1hd Dimer

We obtained milligram quantities of a complex between the head domain of Smc1 (Smc1hd) and the most C-terminal 115 amino acids of Scc1 (Scc1-C) by coexpression in insect cells using the baculovirus system. Crystallization in the presence of ATPγS and magnesium yielded diffraction-quality crystals whose structure was solved using multiple isomorphous replacement (see Supplemental Table S1 at http://www.molecule.org/cgi/content/full/15/6/951/DC1). The resulting structure at 2.9 Å resolution is of good quality (Figure 1G; Table 1).

The yeast Smc1hd domain (Figures 1A–1C) closely resembles published structures of *P. furiosus* Rad50hd (1F2U [Hopfner et al., 2000]; rms deviation 2.4 Å over 239 Cα atoms) and *T. maritima* SMChd (1E69 [Löwe et al., 2001]; rms deviation 2.3 Å over 232 Cα atoms). The Smc1 head forms an ABC ATPase fold in which one of the two β sheets is composed of strands from N- and C-terminal SMC chains (for secondary structure assignments, see Figure 1E). Our structure reveals how the coiled-coil segments are attached to the globular head domain: the loop between S9 and S10 stabilizes outgoing and incoming helices of the coiled coil, and the two coiled coils are attached to the globular head dimer in an almost parallel orientation (Figures 1B and 1C). The Smc1hd structure contains two disordered regions: the N-terminal chain is disordered between residues 55 and 88, while the C-terminal chain is disordered between residues 1084 and 1094 (HE to S9). The loop between residues 55 and 88 contains a short helix and has only been partially built using residual density and a dimeric SMChd structure (Lammens et al., 2004) as a guide.

Our finding that Smc1hd homodimerizes in the presence of ATPγS (Figure 1) and ATP (see below) was unexpected. Presumably, Smc1 heads would normally associate with Smc3 heads in the presence of ATP because hinge-mediated heterodimerization of Smc1 and Smc3 would ensure a high local concentration of heterotypic head domains. Smc1 head dimerization might merely reflect the fact that eukaryotic SMC head domains have not lost their ability to self-dimerize following the ancient gene duplication that gave rise to heterodimeric SMC proteins in eukaryotic lineages from the homodimeric bacterial versions. At present, it is unknown whether Smc1 and Smc3 heads form similar, if not more stable, heterodimers. Independent of the interaction between Smc1 and Smc3, it is nevertheless conceivable that under certain circumstances ATP-mediated interaction of adjacent cohesin complexes via their Smc1 heads creates a more robust form of cohesion than that produced by isolated cohesin complexes.

The Smc1hd Dimer Is a Functional ATPase

The dimer formed by Smc1hd is structurally very similar to that formed by Rad50hd (Hopfner et al., 2000) and by an ABC ATPase transporter (Smith et al., 2002). Crucially, the ABC signature motif on one Smc1hd interacts with the phosphates of a nucleotide bound to a Walker A motif in its partner. ATPγS is sandwiched between the two Smc1hd domains (Figures 1A and 1F). Not surprisingly, residues forming the Smc1hd dimer interface and contacting the ATP molecules are highly conserved among SMC proteins (Figure 3A). Dimerization in this manner is thought to create a pair of sites capable of ATP hydrolysis. In ABC transporters and Rad50, mutation of a conserved serine in the signature motif (equivalent to Smc1's S1130) abolishes contact to the nucleotide phosphates, ATP-dependent dimerization, and hence also ATP hydrolysis, while mutation of a conserved glutamate residue in the Walker B motif (equivalent to Smc1's E1158) compromises ATP hydrolysis without adversely affecting dimerization (Moncalian et al., 2004, Smith et al., 2002). Though ATPase activity associated with cohesin has not hitherto been measured, mutation of the conserved signature motif serine residue or the Walker B glutamate residue of either Smc1 or Smc3

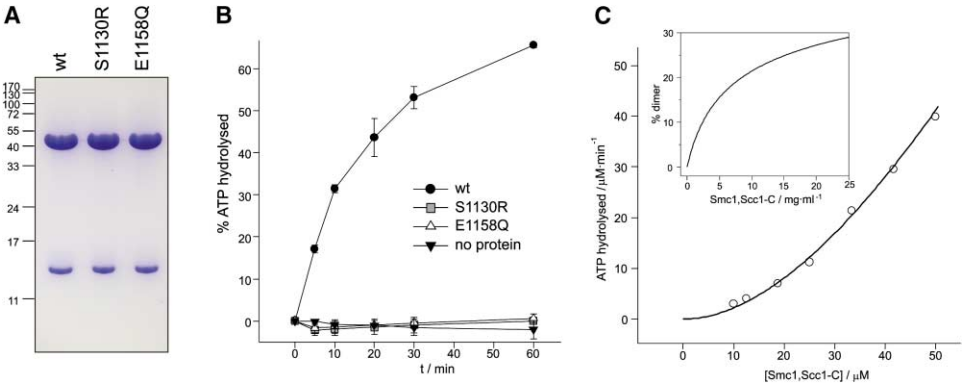

Figure 2. The Smc1hd/Scc1-C Dimer Is a Functional ATPase

(A) SDS-PAGE Coomassie stain of Smc1hd/Scc1-C protein preparations used in the ATPase. The upper band corresponds to Smc1hd, the lower to Scc1-C.

(B) ATPase assay. α^{32}P-labeled ATP and ADP were resolved by thin layer chromatography, and intensities of ADP to ADP+ATP signals were plotted for each time point.

(C) ATPase assays were performed for different protein concentrations of Smc1hd/Scc1-C. ATP hydrolysis rates determined from the linear reaction range for each protein concentration are plotted against the molar protein concentration calculated using a molecular mass of 58.8 kDa (monomeric Smc1hd/Scc1-C). A curve fitting the data was calculated, assuming that the hydrolysis rate is straight proportional to the dimer concentration (Nikaido et al., 1997). This gives a dissociation constant K_d of two Smc1hd/Scc1-C monomers of 260 μM and a rate constant of 7 min^{-1} for the hydrolysis reaction. The low rate constant is consistent with the notion that cohesin's ATP hydrolysis acts as a conformational switch rather than as an active motor. The inset shows the proportion of dimers at different protein concentrations calculated using a K_d of 260 μM.

abolishes cohesin's ability to associate with chromosomes in vivo (Arumugam et al., 2003; Weitzer et al., 2003).

We purified Scc1-C coexpressed with either wild-type, signature motif mutant S1130R, or Walker B motif mutant E1158Q Smc1hd protein in insect cells by affinity chromatography followed by gel filtration. Most complexes eluted from the column with a retention volume consistent with a monomeric 58.8 kDa molecular weight, but a sizeable fraction ($\sim$20%) of the E1158Q mutant complex eluted with a retention volume consistent with a dimeric 117.6 kDa molecular weight (data not shown), implying that a fraction of the mutant protein is trapped in the ATP-bound dimer form because it is unable to hydrolyze the bound nucleotides. We then used the purified Smc1hd/Scc1-C complexes (Figure 2A) in an ATPase assay. ATP was hydrolyzed by wild-type, but not by S1130R or E1158Q, complexes (Figure 2B). Two lines of evidence suggest that ATP hydrolysis is mediated by the sort of dimeric structures seen in our crystals. First, ATP hydrolysis is abolished by the S1130R mutation. Second, we measured a nonlinear increase in ATP hydrolysis with increasing Smc1hd/Scc1-C complex concentration (Figure 2C). Our curves are consistent with the notion that hydrolysis is mediated by dimers and that the dissociation constant (K_d) between two Smc1hd/Scc1-C complexes is in the 10^{-1} mM range, which is comparable to the K_d estimated by similar means for the ABC ATPase domains of the HisP transporter (Nikaido et al., 1997).

We conclude that the Smc1hd/Scc1-C complex crystallizes in a manner compatible with ATP hydrolysis. Importantly, association of Scc1-C with the underside of the Smc1 head does not appear to compromise formation of hydrolysis-competent dimeric structures. This latter finding is difficult to reconcile with the recent proposal that Scc1's C-terminal separase cleavage product prevents interaction of Smc1 and Smc3 heads (Weitzer et al., 2003). However, we cannot yet exclude the possibility that Smc3 heads might have additional protruding domains which would prevent them from dimerizing with Smc1 heads bound by Scc1-C or that the presence of Scc3 bound to the larger C-terminal Scc1 fragment produced by separase cleavage hinders Smc1-Smc3 head dimerization in vivo.

Scc1-C Is a Winged Helix Domain

Kleisins contain at their N- and C termini conserved globular domains (Schleiffer et al., 2003) that in the case of Scc1 bind Smc3 and Smc1 heads, respectively, and thereby connect them through a mechanism distinct from ATP-mediated SMC head dimerization (Gruber et al., 2003; Haering et al., 2002). Our structure shows that the most C-terminal $\sim$80 residues of yeast Scc1 form a winged helix domain (WHD) (reviewed in Gajiwala and Burley, 2000) that binds to the Smc1 head. The first 32 N-terminal amino acids (451–482) and a small loop region (513–520) of Scc1-C are disordered (Figure 1E). The ordered domain corresponds almost exactly to the boundaries and secondary structure predicted by sequence conservation of kleisins (Schleiffer et al., 2003), implying that the C-terminal domains of all members of the kleisin superfamily may form WHDs that bind to SMC heads in the manner observed in our Smc1hd/Scc1-C structure.

WHDs usually contain three helices followed by two β strands and have been classified as a subgroup of helix-turn-helix proteins. Most but not all participate in site-specific DNA (or RNA) binding, using helix H3 to recognize base pairs within DNA's major groove. Many WHD proteins were found in a DALI search for known structures similar to the C-terminal domain of Scc1. The protein with the highest structural similarity ($Z = 9.0$) is

the *S. aureus* SarS protein (1P4X [Li et al., 2003]) known to bind promoters of specific genes. SarS actually contains two WHDs, one at its N terminus and a second at its C terminus (Figure 1D). Interestingly, the two winged helices from SarS have a spacing and relative orientation similar to the two winged helices associated with each Smc1hd dimer. A crucial difference is that the surfaces on SarS and other WHDs predicted to bind to DNA are occupied instead by the Smc1 head in Scc1-C (Figures 1C and 1D). This and experimental evidence (see below) indicate that Scc1-C's winged helix does not participate in DNA binding. Scc1-C is not unique in binding protein and not DNA. For example, the second highest hit from the DALI search, iso-flavone-o-methyltransferase (1FPX [Zubieta et al., 2001]), uses its WH domain for dimerization.

The structure of SarS raises the possibility that Scc1's N-terminal domain might also be a winged helix domain. Sequence alignments and secondary structure analyses suggest a similarly sized domain at the N termini of kleisin proteins, containing three helices that might form a helix-turn-helix motif but, at least in the case of ScpA, missing the two β strands forming the "wing" in WHD proteins (Schleiffer et al., 2003). If the N-terminal domain of Scc1 folds into a helix-turn-helix motif, then its recognition helix might bind Smc3 in a manner similar to the C-terminal WHD binding Smc1. It is therefore conceivable that the broad outlines of Scc1's interaction with Smc1/3 heterodimers have already emerged from our Smc1hd/Scc1-C structure.

Does the Scc1-C WHD Bind DNA?

When bound to Smc1 heads, Scc1's C-terminal winged helix is unlikely to bind DNA in a fashion similar to other winged helix DNA binding domains. The interface between Scc1-C and Smc1hd is almost exclusively hydrophobic and lacks the positively charged residues often found in winged helices involved in binding DNA (Figure 3B). It is nevertheless striking that our Smc1hd/Scc1-C structure contains a positively charged patch associated with the inner surfaces of each WH domain (Figure 3C). To test its biological importance, we generated yeast strains expressing Scc1 proteins in which the residues generating the patch, namely K509, K521, R522, and R526, were mutated. Mutant proteins were expressed from the native *SCC1* promoter at levels comparable to wild-type protein, as judged by immunoblotting against their C-terminal HA_3-epitope (Figure 4B). The strains expressed in addition a wild-type copy of the *SCC1* gene under control of the galactose-inducible and glucose-repressible *GAL1-10* promoter. The mutant Scc1 proteins were tested for their ability to sustain proliferation in the absence of wild-type Scc1 on glucose media. Surprisingly, all strains expressing mutant proteins grew at a rate similar to the strain expressing the wild-type protein, even at 37°C (Figure 4B). The complex between Smc1 and Scc1-C has one other notable patch of positive charge (right hand side of Figure 3D). This is the region on Smc1hd where a long loop and a small helix between helix HA and β strand S4 are disordered (residues 55–88), and the electrostatic potential was calculated using only ordered residues. The loop is long and it is possible that some residues reach down to Scc1-C. Importantly, residues in this loop are close to the nucleotide and could couple Scc1-C binding with hydrolysis. However, the disorder makes it difficult to design specific mutants to test this hypothesis.

The only indication that Smc1hd/Scc1-C complexes might interact with DNA is our observation that their ATPase activity was increased, albeit only 2.5-fold, upon addition of 25 nM 3.5 kb circular supercoiled or linear plasmid DNA to 25 μM Smc1hd/Scc1-C. Addition of excess heparin or single stranded oligonucleotide DNA had little or no effect (data not shown).

The Interaction of Scc1 with Smc1 Is Essential

The major contacts between Smc1 and Scc1's WHD are made by the latter's "recognition helix" and "wing" binding to the two most C-terminal β strands (S14 and S15) of Smc1's head (Figure 1E). Contacts are largely hydrophobic and involve residues F528 and L532 from the WHD recognition helix and residues L1201, G1203, Y1205, I1216, and L1218 from Smc1's S14 and S15 (Figure 4A). The interaction is stabilized by a contact between the side chain of Q544 from the WHD wing and the backbone of Smc1's strand S15, and by contacts between the WHD recognition helix and residues N1192, F1195, and E1196 from Smc1's helix HH and residue I32 of Smc1's strand S3 immediately preceding the P loop (Figure 4A). Residues in Scc1's recognition helix and wing, which together form the pocket that binds Smc1, are highly conserved among all kleisin proteins (Figure 3B). Smc1's preference for binding Scc1's C- rather than N terminus is presumably determined by these conserved residues. It is harder to detect such a conserved patch within predicted S14 and S15 strands from various SMC proteins (Figure 3C), but it is notable that residues equivalent to Y1205 within Smc1's S14 strand are conserved among SMC proteins thought to bind the C-terminal domain of kleisins, namely Smc4 and Smc1 proteins. The equivalent residue in Smc2 and Smc3 proteins is frequently lysine or arginine.

To confirm that Scc1 does indeed bind to Smc1 in the manner revealed in our Smc1hd/Scc1-C structure in vivo, we mutated the side chains of three amino acids in Scc1's WHD (F528, L532, and Q544) that make major contacts to the Smc1 head. All three residues are highly conserved in kleisin proteins (Schleiffer et al., 2003). We tested mutant Scc1 proteins for their ability to sustain growth in glucose medium of yeast cells whose sole wild-type *SCC1* gene is expressed from the *GAL1-10* promoter. Despite accumulating to normal levels, F528R and L532R proteins failed to sustain growth at any temperature tested, while Q544K sustained only poor growth at 25°C and none at 30°C or higher (Figure 4C). To address whether the mutant proteins are dysfunctional because they cannot bind Smc1 stably, we expressed the mutant proteins tagged with an HA_3 epitope in strains whose Smc1 protein was tagged with a myc_{18} epitope. Immunoprecipitation of the tagged proteins showed that the interaction between Scc1 and the Smc1/3 dimer was strongly reduced by F528R, L532R, and Q544K mutations (Figure 4D).

We also investigated the importance of Smc1's Y1205 residue by expressing mutant or wild-type Smc1-myc_9 protein as an additional copy in cells that expressed

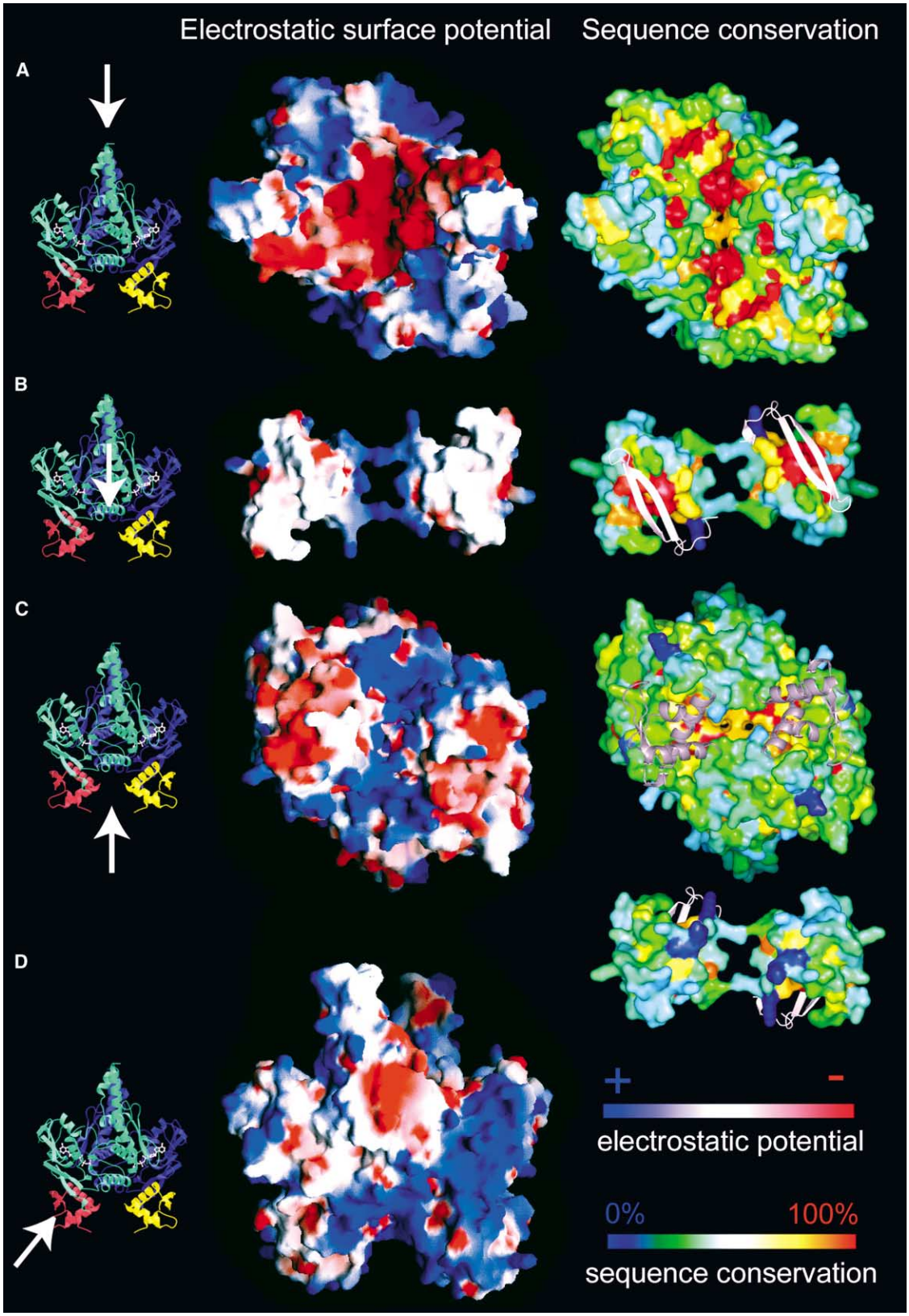

Figure 3. Electrostatic Surface Potential Maps (±6 keT) and Sequence Conservation Plots

Conservation of surface residues was calculated using alignments of eukaryotic Smc1-6 protein families or eukaryotic α-γ and bacterial kleisin families, respectively.

(A) Top view along the coiled coils. The active sites in the Smc1hd dimer are surrounded by negative charge, and residues surrounding

Scc1 tagged with the HA_6 epitope and compared the amounts of Scc1-HA_6 coimmunoprecipiated with Smc1-myc_9. Substitution of Y1205 by lysine completely abolished the interaction between Smc1/3 dimers and Scc1, while substitution by alanine reduced but did not abolish the interaction (Figure 4E). The effect of Y1205A is more evident when comparing the amounts of C-terminal Scc1 cleavage fragment coimmunoprecipitated by mutant and wild-type Smc1/3 dimers. This suggests that the Y1205A mutation is compatible with Scc1-C binding the Smc1 head and with subsequent formation of contacts between Scc1-N and the Smc3 head but that the mutation compromises the interaction between Scc1-C and Smc1 when this is not stabilized by tripartite ring formation. To evaluate the effect of Y1205K and Y1205A mutations on cohesin function, we integrated an ectopic copy of either wild-type or mutant *SMC1* genes in a diploid strain in which one copy of the endogenous *SMC1* genes had been deleted. Tetrad dissection after sporulation showed that Y1205A, but not Y1205K, was able to sustain cell division (data not shown).

Remarkably, disruption of the Scc1-Smc1 interaction is sufficient to abolish all interaction with Smc1/3 heterodimers even though Scc1 also interacts stably with Smc3. This is consistent with the finding that the N terminus of Scc1 cannot bind to Smc3 heads in yeast when not attached to its C terminus (Arumugam et al., 2003). The implication is that binding of Scc1's N terminus to Smc3 depends on the prior binding of its C terminus to Smc1. Interestingly, we could not detect C-terminal separase cleavage fragments from the three mutant Scc1 proteins incapable of binding the Smc1/3 heterodimer (Figures 4C and 4D). There are two explanations for this: either Scc1 that is not bound to Smc1 is incapable of associating with chromosomes and is therefore a poor substrate for separase, or (albeit less likely) the C-terminal cleavage product is more rapidly degraded when not bound to the Smc1 head.

Notably, serine 525 is replaced by asparagine in the two *scc1* alleles (*scc1-73* and *scc1-312*) originally isolated in a screen for yeast mutants with defective sister chromatid cohesion (Michaelis et al., 1997; V.L. Katis, personal communication). As expected, yeast cells expressing only S525N Scc1 protein grew at 25°C but not at 37°C (Figure 4F). S525 is situated in the WHD recognition helix, and its side chain faces toward the Smc1 head domain (Figure 4A). To test whether the S525N mutation weakens the contact between Scc1-C and Smc1, we grew cells expressing Smc1 tagged with myc_{18} and an extra copy of either wild-type or S525N Scc1 tagged with HA_3 at 23°C or at 37°C. The amount of Scc1-HA_3 bound to Smc1/3 was strongly reduced by the S525N mutation when cells were grown at 37°C, but not at 23°C (Figure 4F). Sister chromatid cohesion established by S525N Scc1 when *scc1-73* cells undergo DNA replication at the permissive temperature (25°C) is largely destroyed by shifting G2 or M phase cells to the restrictive temperature (37°C) (Ciosk et al., 2000). This implies that the interaction of Scc1's C terminus with Smc1 heads is required for maintaining cohesion between sister chromatids as well as for generating functional cohesin complexes. This is an important prediction of the ring hypothesis, which postulates that any disruption of tripartite cohesin rings should abolish sister chromatid cohesion.

Interestingly, Scc1's winged helix binds Smc1's head in close proximity to its ATPase active site. Residues F529, S533, and T536 in the WH recognition helix (Figure 4A) contact the P loop (Walker A motif) that binds the phosphates of the nucleotide. To test whether these contacts are of physiological relevance, we analyzed the effect of substituting these residues with alanine. Yeast cells expressing only mutant proteins were viable at all temperatures tested (Figure 4C), though the S533A mutant grew slightly slower than wild-type at 25°C. It has been shown that point mutations in Smc1's Walker A or B motifs that abolish ATP binding dramatically reduce Scc1's ability to bind stably to Smc1/3 heterodimers in vivo (Arumugam et al., 2003; Weitzer et al., 2003). Our structure gives little or no explanation for these findings. When the structure of the monomeric, ATP-free SMC head domain of *T. maritima* (1E69 [Löwe et al., 2001]) and our Smc1hd/Scc1-C dimer structure are superimposed, few if any structural differences can be seen in the area of the SMC head domain to which Scc1 binds, namely the region around β strands S14 and S15. The ATP-free form of the Smc1 head should therefore be compatible with binding Scc1's C terminus. It might nevertheless be possible that the loop between residues 55 and 88 that is disordered in our structure and also partially in the *Tm*SMC structure blocks Smc1's Scc1 binding site in the absence of nucleotide. Bound ATP might in addition stabilize the Smc1 head structure, in particular the P loop in the vicinity of the Scc1 binding site. Alternatively, the presence of Scc3 might influence the manner through which Scc1's WHD binds Smc1's head so that it depends on nucleotide binding. The activity of additional factors (e.g., Scc2/4) might also modulate this interaction in vivo.

Is There Any Turnover of Cohesin Subunits in Complexes that Have Formed Cohesion?

Having analyzed the physical interaction between Scc1 and SMC ATPase heads, we next assessed the stability of this interaction when cohesin holds sister chromatids together inside cells. According to the ring model, cohesin holds sister DNA molecules together by entrapment inside its tripartite ring structure. If cohesin's klei-

the nucleotide are highly conserved. Another patch of highly conserved residues is located in the pocket that holds the disordered loop residues 55–88.

(B) Top view onto Scc1-C. The interface between Scc1-C and Smc1 is mostly hydrophobic, and Scc1-C's cleft holding Smc1 strands S14 and S15 is highly conserved. Smc1's β strands S14 and S15 are shown in light gray.

(C) Bottom view. The cleft between the two Scc1-C domains is positively charged. Smc1's Scc1-C interacting surface (top) and the outside surface of Scc1-C (bottom) are poorly conserved. Scc1's WHD domain is shown in dark gray.

(D) Side view. A large positively charged patch is created on a surface at the interface of Smc1hd and Scc1-C, very close to the active site.

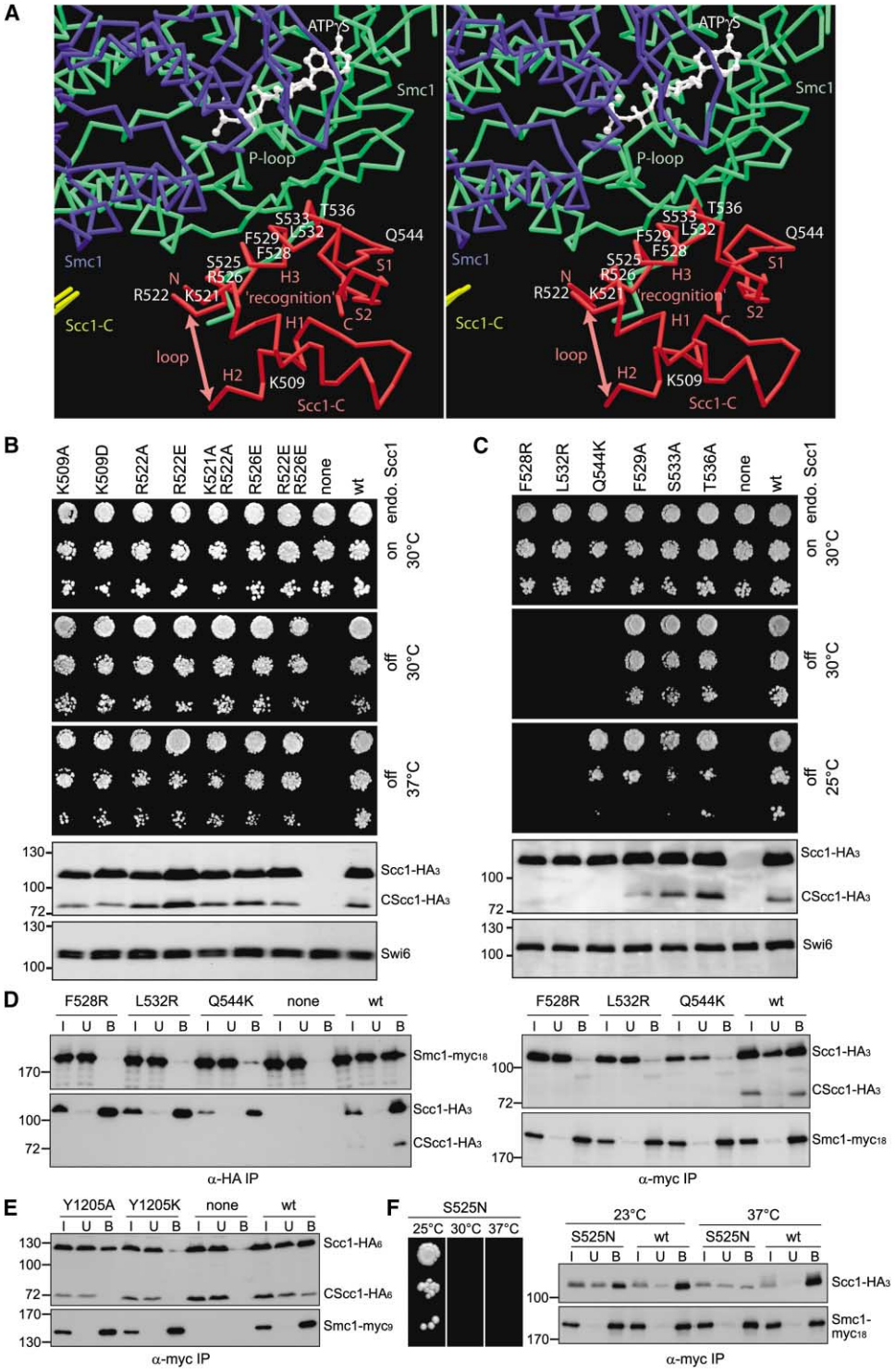

Figure 4. The Scc1-C Winged Helix Domain Makes the Essential Contact to the Smc1 Head

(A) Stereo plot of the Smc1/Scc1-C interaction interface. The WHD recognition helix (H3) contains most of the Scc1-C contacts. Residues mutated in this study are labeled. Scc1-C binds directly to the P loop of the Smc1 active site.

(B and C) Analysis of Scc1 mutants for functionality in vivo. Yeast strains K12449-61 and K12589-91 (*MAT*α, *GAL1-10-SCC1::KITRP1, leu2::SCC1-(mut, TEV$_{268}$)-HA$_3$::LEU2*) express the mutant *SCC1* gene from its native promoter and a wild-type *SCC1* gene from the *GAL1-10* promoter. All strains grow on galactose media to maintain the expression of wild-type *SCC1* (top). When expression of wild-type *SCC1* is repressed on glucose media, cells can only grow if the mutant *SCC1* is functional (middle, bottom). Immunoblotting against the HA$_3$-epitope shows expression of mutant Scc1 proteins at levels comparable to the wild-type protein. Note that no C-terminal separase cleavage product of Scc1 is seen for mutants F528R, L532R, and Q544K. Swi6: loading control.

(D) Scc1 mutants F528R, L532R, and Q544K fail to associate stably with Smc1/3 dimers in vivo. Strains K12564-68 (*MAT*α, *SMC1-myc$_{18}$::KITRP1,*

sin subunit would frequently dissociate from SMC heads post replication, it might have the same effect as its proteolytic cleavage, namely escape of DNA strands from their entrapment inside rings. In this case, separase-resistant Scc1 molecules expressed after DNA replication should be able to exchange with cleavable Scc1 molecules in cohesin complexes which had formed during DNA replication. Thus, noncleavable tripartite rings would continue to hold sister chromatids together after cells had activated separase. In principle, such noncleavable cohesive structures could of course also be produced by the de novo formation of fully new structures if this were also possible post replication. We therefore analyzed the consequences of expressing noncleavable Scc1 (Uhlmann et al., 1999) in cells arrested in metaphase by depletion of the APC/C activator protein Cdc20. If noncleavable Scc1 were incapable of blocking the onset of anaphase upon restoration of Cdc20 synthesis, then we could conclude that it can neither produce new structures nor exchange into old ones during metaphase.

We created yeast strains in which HA_3-tagged wild-type or noncleavable Scc1 was expressed under control of the *GAL1-10* promoter in cells with an endogenous *SCC1* gene tagged with myc_{18}. A third strain expressed Scc1-HA_3 from the endogenous *SCC1* promoter. The sole copy of Cdc20 in all three strains was expressed under control of the methionine-repressible *MET3* promoter, making a reversible metaphase arrest possible. Cells growing logarithmically in the presence of raffinose (*GAL1-10* off) and in the absence of methionine (Cdc20 on) were shifted to methionine-containing medium (Cdc20 off). After most cells had accumulated in metaphase, we induced synthesis of wild-type or noncleavable Scc1-HA_3 protein by addition of galactose. Chromosome spreading showed that within 3 hr of the addition of galactose, the amount of Scc1-HA_3 protein made from the *GAL1-10* promoter that had bound to chromosomes was comparable to the amount of Scc1-HA_3 made from its native *SCC1* promoter (Figure 5A). When whole-cell extracts were centrifuged through a sucrose cushion, most Scc1-HA_3 was recovered in the chromatin-containing pellet fraction, while little or no Scc1-HA_3 could be detected in the soluble fraction (Figure 5A). Both results show that Scc1-HA_3 readily associates with chromosomes when expressed during the metaphase arrest.

Cdc20 synthesis was restored by shifting cells to medium lacking methionine, and further expression from the *GAL1-10* promoter was prevented by replacement of galactose by glucose. This led to separase activation, which was monitored by the disappearance of Scc1-myc_{18} from chromosome spreads (Figure 5B) and its transient cleavage (Figure 5E). Scc1-myc_{18} reappeared on chromosomes by the onset of DNA replication in the following cell cycle and disappeared once again after a second round of separase cleavage. Wild-type Scc1-HA_3 protein expressed from *GAL1-10* disappeared from chromosomes with similar kinetics to endogenous Scc1-myc_{18}, but due to repression of *GAL1-10* it did not reappear (Figure 5B). Cells that had expressed wild-type Scc1-HA_3 during the Cdc20 arrest exited metaphase and rapidly underwent anaphase (Figure 5C). Both the onset of DNA replication (data not shown) and the onset of the second anaphase (Figure 5C) were modestly delayed relative to the strain expressing Scc1-HA_3 from the *SCC1* promoter, possibly because larger than normal amounts of Scc1 cleavage fragments may interfere with ubiquitin-mediated degradation of the Cdk1 inhibitor Sic1.

Noncleavable Scc1-HA_3 protein, in contrast, remained tightly associated with chromosomes for at least 3 hr after the resumption of Cdc20 synthesis (Figure 5B). Remarkably, it neither prevented nor even delayed the onset of the first anaphase (Figure 5C). Cells separated sister chromatids with identical kinetics to those that had expressed wild-type Scc1-HA_3, be it from the *SCC1* or the *GAL1-10* promoter. Nevertheless, noncleavable Scc1-HA_3 completely blocked a second anaphase, despite there having been no further synthesis of the protein after restoration of Cdc20 synthesis. The cells clearly attempted to undergo a second anaphase because the second round of Scc1-myc_{18} cleavage and disappearance from chromosomes occurred despite the persistence of noncleavable Scc1-HA_3. In summary, noncleavable protein made exclusively during a metaphase arrest caused by Cdc20 depletion blocks the second, but not the first, round of anaphase following the resumption of Cdc20 synthesis.

To exclude the possibility that the failure of noncleavable Scc1-HA_3 to block the first anaphase is not due to some unforeseen property associated with the experimental protocol used to reversibly arrest cells in metaphase, we checked whether anaphase would be blocked if noncleavable Scc1-HA_3 were expressed prior to DNA replication. To do this, we added α factor to cells growing in the absence of methionine and galactose. After most cells had arrested in G1, they were transferred to medium containing both galactose (to induce expression of either wild-type or noncleavable Scc1-HA_3) and methionine (to arrest cells in metaphase after they had completed DNA replication). When most cells had arrested in metaphase, we restored Cdc20 synthesis by

leu2::SCC1(mut, TEV_{268})-HA_3::LEU2) express an additional copy of the mutant *SCC1* gene from its native promoter. Coimmunoprecipitation of Smc1-myc_{18} with Scc1-HA_3 (left) and of Scc1-HA_3 with Smc1-myc_{18} (right) was tested by immunoblotting input (I), unbound (U), and bound (B, 3×) fractions.

(E) Mutation of Smc1 residue Y1205 reduces Smc1's affinity to Scc1. Extracts were prepared from strain K12929-31 (*MAT*α, *SCC1-HA_6::HIS3, ura3::SMC1(mut)-myc_9::URA3*) or K7563 (*MAT*α, *SCC1-HA_6::HIS3*), and Smc1/3 was immunoprecipitated by the myc_9 epitope on (mutant) Smc1. Coimmunoprecipitation of Scc1-HA_6 and its C-terminal separase cleavage fragment was detected by immunoblotting against the HA_6 epitope.

(F) The temperature sensitivity of *scc1-73* (S525N Scc1) is caused by its reduced affinity to Smc1/3 at high temperatures. Functionality of S525N Scc1 in vivo was tested for strain K12927 on glucose-containing media as described in (B). Strains expressing wild-type (K12567) or S525N mutant (K12926; *MAT*α, *SMC1-myc_{18}::KlTRP1, leu2::SCC1(S525N, TEV_{268})-HA_3::LEU2*) Scc1-HA_3 protein were either grown at 23°C or 37°C before extract preparation and immunoprecipitation of Smc1-myc_{18}. Coimmunoprecipitation of Scc1-HA_3 was probed by immunoblotting against HA_3.

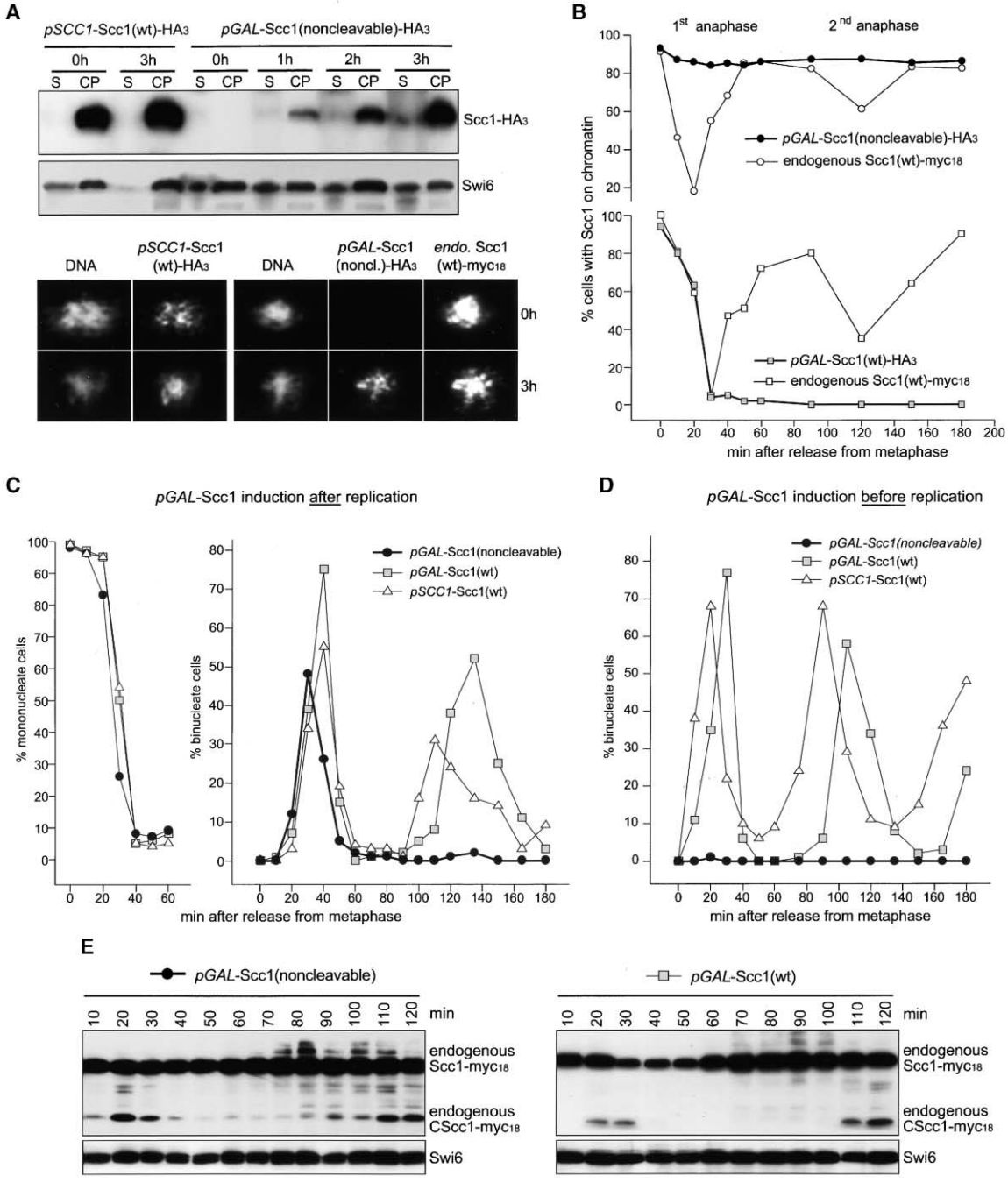

Figure 5. No Scc1 Turnover in Chromosomal Cohesin Complexes during Metaphase

(A) Strain K11733 (*MATa, SCC1-HA$_3$::HIS3, pMET3-CDC20::natMX4*) expresses Scc1-HA$_3$ epitope from its native promoter. Strain K11732 (*MATa, SCC1-myc$_{18}$::KITRP1, pGAL1-10-SCC1(R$_{180}$D, R$_{268}$D)-HA$_3$::LEU2, pMET3-CDC20::natMX4, his::TetR-GFP::HIS3, ura3::TetO112::URA3*) expresses a separase noncleavable version of Scc1-HA$_3$ from the *GAL1-10* promoter. Both strains were arrested in metaphase by repressing Cdc20 expression from the *MET3* promoter. After cells had arrested, the *GAL1-10* promoter was induced, and Scc1-HA$_3$ levels in soluble fractions (S) and chromatin pellets (CP) were determined by immunoblotting against the HA$_3$ epitope (top), or Scc1-HA$_3$ levels on chromatin were detected by in situ immunofluorescence staining (bottom) at successive time points. Three hours after induction, the amount of Scc1-HA$_3$ on chromatin when expressed from *GAL1-10* was comparable to Scc1-HA$_3$ when expressed from its native promoter.

(B) Expression of noncleavable Scc1-HA$_3$ (K11732) or wild-type Scc1-HA$_3$ (K11731; *pGAL1-10-SCC1(wt)-HA$_3$::LEU2*, otherwise isogenic to K11732) from the *GAL1-10* promoter was stopped, and Cdc20 expression was induced to release cells from metaphase. At consecutive time points, chromosomal spreads were probed for Scc1-HA$_3$ (closed circles, closed squares) and endogenous Scc1-myc$_{18}$ (open circles, open squares).

(C) The percentage of cells in metaphase (mononucleate cells, left) or undergoing anaphase (binucleate cells, right) is plotted for each time point after Cdc20 induction for cells which had expressed noncleavable (closed circles) or wild-type Scc1-HA$_3$ (closed squares) during the arrest from *GAL1-10,* or expressed Scc1-HA$_3$ from its native promoter (open triangles).

(D) Strains K11731-33 were arrested in G1 by α factor and then released into media containing galactose to induce expression from *GAL1-10*

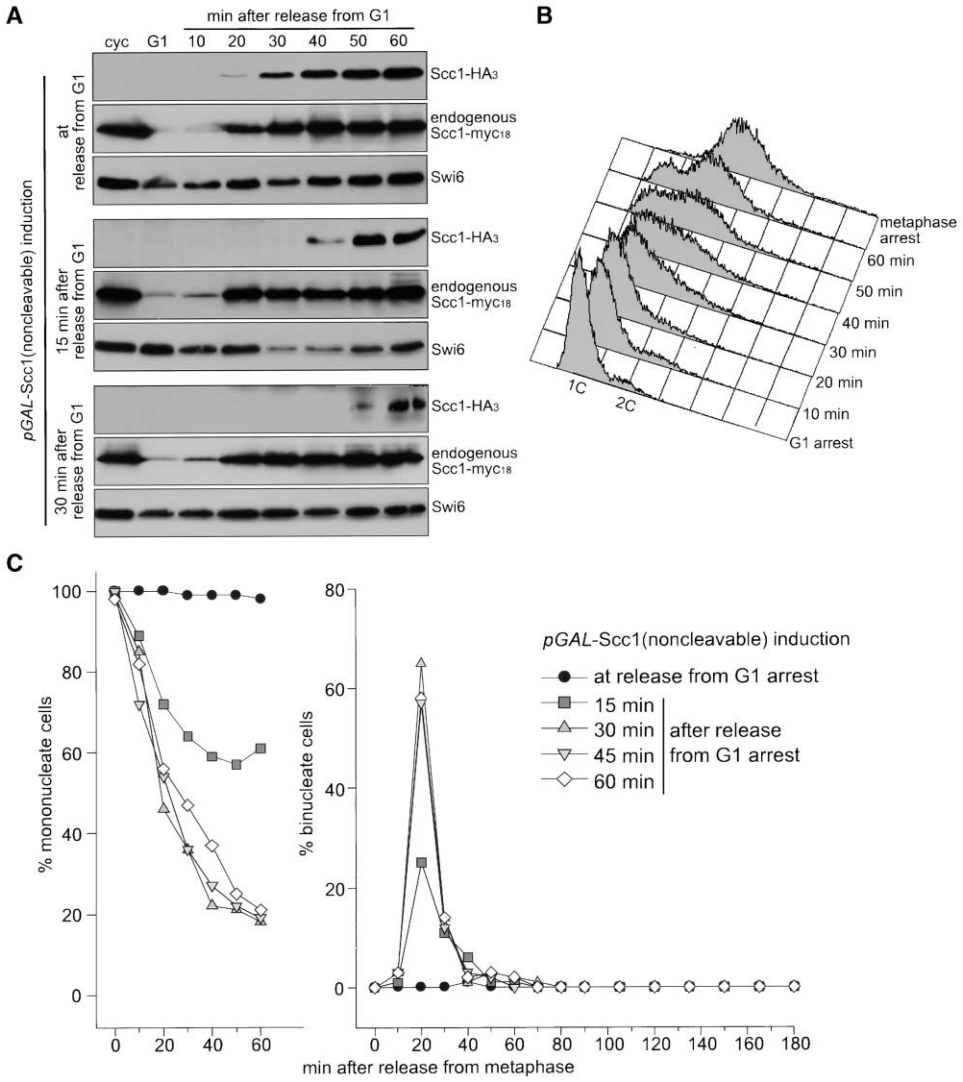

Figure 6. No Exchange of Scc1 in Chromosomal Cohesin Complexes after DNA Replication

Strain K11732 was arrested in G1 by α factor. Cells were then synchronously released into media containing methionine to rearrest them in metaphase. Expression of noncleavable Scc1-HA_3 from *GAL1-10* was induced by addition of galactose at the indicated time points after release. (A) Scc1-HA_3 expression was detectable by immunoblotting against HA_3 20–30 min after galactose addition. Endogenous Scc1-myc_{18} was detectable $\sim$20 min after release from G1 arrest.

(B) FACScan analysis shows that cells started to undergo DNA replication 20–30 min and largely completed replication 60 min after the release.

(C) Cdc20 expression was induced after cells had rearrested in metaphase. The percentage of cells in metaphase (mononucleates, left) or undergoing anaphase (binucleates, right) is plotted for each time point after the release for cells whose expression of noncleavable Scc1-HA_3 had been induced at the time of release from G1 (closed circles), or 15 (closed squares), 30 (closed right-side-up triangles), 45 (closed upside-down triangles), or 60 (open diamonds) min after release from G1. As expression of the noncleavable Scc1 from *GAL1-10* continued, cells failed to undergo a second anaphase.

shifting cells into methionine-free media containing glucose and examined whether cells underwent anaphase. As expected, cells that had expressed wild-type Scc1-HA_3 from the *GAL1-10* promoter underwent anaphase as synchronously as cells that had expressed it only from the *SCC1* promoter, but cells that had expressed noncleavable Scc1-HA_3 from the *GAL1-10* promoter failed to do so completely (Figure 5D).

To test whether there is exchange or generation of new bridges at any period from the completion of DNA

and methionine to rearrest them in metaphase. Cells were released from metaphase by Cdc20 induction. The percentage of cells undergoing anaphase is plotted for strains expressing noncleavable (closed circles) or wild-type Scc1-HA_3 (closed squares) from *GAL1-10* or from its native promoter (open triangles).

(E) Whole-cell extracts of strains 11732 and 11732 were prepared at time points following release from metaphase, and cleavage of endogenous Scc1-myc_{18} was monitored by probing immunoblots for myc_{18}.

replication until metaphase, we repeated the above experiment but induced synthesis of noncleavable Scc1-HA_3 at different times after release from the α factor arrest. Following accumulation in G1, cells were transferred to pheromone-free medium containing methionine (Cdc20 off), and the cultures were split into five aliquots, to which galactose was added at different times, specifically at 0, 15, 30, 45, and 60 min after pheromone release. DNA replication took place with similar timing in all five cultures as monitored by measuring DNA content per cell by FACScan (Figure 6B). The kinetics with which noncleavable Scc1-HA_3 protein actually accumulated was measured by immunoblotting (Figure 6A). In general, addition of galactose led to accumulation of detectable Scc1-HA_3 levels about 25 min later. When galactose was added at the time of release from pheromone arrest, protein accumulated at the onset of DNA replication, when added 15 min later, it accumulated as many of the cells were half way through S phase, and when added 30 min after release, it accumulated only after many cells had nearly completed replication. Wild-type Scc1-myc_{18} protein expressed from its native promoter accumulated $\sim$20 min after release (Figure 6A), that is, shortly before the onset of S phase.

When cells had completed DNA replication and arrested in metaphase (3 hr after release from the α factor arrest), they were transferred to medium lacking methionine and galactose to test whether they were capable of separating sister chromatids upon the resumption of Cdc20 synthesis. Addition of galactose at the time of release from pheromone arrest prevented anaphase in all cells, addition 15 min later prevented anaphase in about half of the cells, and addition 30 min after release or later blocked very few if any cells (Figure 6C). Noncleavable Scc1 expressed any time after DNA replication has largely taken place therefore doesn't block sister chromatid separation. We conclude that noncleavable protein neither replaces cleavable Scc1 protein currently engaged in holding sister chromatids together nor creates new links between sister chromatids.

A Long Lasting Link in the Cohesin Ring

Our observations on the effect of expressing noncleavable Scc1 at different stages of the cell cycle suggest not only that dissociation of Scc1 from Smc1/3 heterodimers that have already formed bridges between sister chromatids is so slow that there is little or no exchange during a 3 hr period but also that cohesion between sister chromatids can only be built during S phase and cannot be reinforced during a normal G2 or M phase. Our experiments extend previous ones showing that Scc1 synthesized after DNA replication cannot form cohesion (Uhlmann and Nasmyth, 1998), because they show that cohesion cannot be generated postreplicatively even when sisters are already held together by preexisting cohesion. Mere proximity of sister DNAs is clearly not sufficient for cohesin to build sister chromatid cohesion. Special mechanisms and enzymes associated only with replication forks may be required to build connections exclusively between sister DNAs. Alternatively, replication forks might pass through cohesin rings. The lack of Scc1 exchange may be due partly to the bivalence of its interaction. If one end of Scc1 dissociates from an SMC head, association of its other end with the opposing head will maintain such a high local concentration that the dissociated end and not some competing molecule will reengage the free SMC head.

By anchoring one half of Scc1 to the Smc1 head, the Smc1hd/Scc1-C complex enables the subsequent interaction of Scc1's N-terminal domain with the Smc3 head, thereby linking the two heads of Smc1/3 heterodimers together to form tripartite rings whose stability may be much greater than the bipartite rings formed by association of SMC heads alone. The persistence of cohesion most probably depends on the stable interconnection of Smc1 and Smc3 heads by Scc1, because severing the connection between N- and C-terminal domains of Scc1 destroys cohesion immediately as does, presumably, disruption of the Scc1-Smc1 interaction due to the temperature-sensitive S525N mutation. The stability of kleisin-SMC interactions within cohesion complexes may be a feature that is unique to cohesin, which unlike condensin can only form functional structures during one period of the cell cycle (S phase) but must use these structures for long periods thereafter, especially during oogenesis when mammalian oocytes are thought to spend many years if not decades in G2 before undergoing the first meiotic division.

Further work is necessary to define whether the Scc1-Smc1 interaction has mechanistic roles beyond serving as a connector between Scc1 and the Smc1/3 heterodimer. Although we do not find obvious effects in vivo of mutations in close proximity to the ATP binding pocket (P loop) of Scc1, we do observe that the C-terminal winged helix does bind in the vicinity of Smc1's P loop region and may therefore regulate Smc1's ATP hydrolysis cycle. The finding that Smc1 mutants deficient in ATP binding have a strongly reduced affinity to Scc1's C terminus in vivo (Arumugam et al., 2003; Weitzer et al., 2003) suggests that the SMC ATPase cycle might in turn regulate the kleisin-SMC interaction. If sister DNAs are trapped within individual tripartite cohesin rings, they could enter these rings either upon transient dissociation of Smc1 and Smc3 hinge domains or when Smc1 and Smc3 heads are not connected by Scc1. If the latter is true and if it is the case that Smc1/3 heterodimers can form tripartite rings prior to sister DNA entrapment, then it must be possible to dissociate Scc1 from Smc1/3 heads, at least transiently, and it has been suggested that the ATP hydrolysis cycle might have a role in this process (Arumugam et al., 2003). In this case, one of the key issues for the future will be to understand whether, and if so how, SMC-kleisin interactions can under some circumstances be labile enough to pass DNAs between SMC heads but under other circumstances be stable enough to maintain sister chromatid cohesin for long periods after DNA replication has been completed.

Experimental Procedures

Expression and Purification of Smc1hd/Scc1-C

Smc1hd is a fusion protein between the N- and C termini of *S. cerevisiae* Smc1 including short stretches of the coiled coil and connected by a 14 amino acid linker (ESSKHPTSLVPRGS). Scc1-C consists of the most C-terminal 115 residues of the *S. cerevisiae* Scc1(Mcd1) protein connected to an N-terminal His_6 tag (MHHHHHH).

Proteins were produced in insect cells by coinfection with recombinant baculoviruses and purified via metal affinity chromatography followed by gel filtration (see Supplemental Material at http://www.molecule.org/cgi/content/full/15/6/951/DC1). Smc1hd/Scc1-C eluted from the gel filtration column in a single peak at V_{ret} ~78 ml, consistent with the apparent molecular weight of an Smc1hd/Scc1-C monomer (58.8 kDa). Peak fractions were concentrated to 15 mg/ml by ultrafiltration. The typical yield from 30 T250 flasks confluent cells was 12–15 mg purified protein.

Crystal Structure of Smc1hd/Scc1-C

Crystallization conditions were found using a 100 nl crystallization setup employing 1200 standard conditions (Stock et al., 2004). 1 μl Smc1hd/Scc1-C complex at 15 mg/ml in 20 mM TRIS-HCl (pH 7.5), 100 mM NaCl, 4.5 mM $MgCl_2$, 5 mM β-mercaptoethanol, 2 mM ATPγS was mixed with 1 μl crystallization solution containing 100 mM sodium acetate (pH 4.6), 9.5% PEG2000, and 15 mM $MgCl_2$. Drops were equilibrated for 1 day at room temperature before ATPγS hydrolysis dissolved the crystals. For generation of derivatives, data collection and analysis see Supplemental Material.

ATPase Assay

Purified Smc1hd/Scc1-C was incubated at a final concentration of 50 μM or at the concentrations plotted in Figure 2C in 20 mM TRIS-HCl (pH 7.5), 100 mM KCl, 10 mM $MgCl_2$, 2 mM ATP, and 25 μCi/ml α^{32}P-ATP at 30°C. At the indicated time points, 1 μl reaction mixture was spotted onto PEI cellulose TLC plates (Merck). TLC plates were developed in 1 M HCOOH, 0.5 M LiCl and exposed to phosphorimager screens. Signal intensities for ATP and ADP spots were quantified using ImageQuant software (Amersham).

Yeast Strains

All strains are derivatives of W303. Genotypes are listed in the figure legends; all epitope tags are C-terminal fusions.

Scc1 and Smc1 Mutant Analysis

Plasmids encoding mutant *SCC1* (see Supplemental Material) were transformed into yeast strain K9514 (*MATα, pGAL1-10-SCC1::KITRP1*) for integration at the *LEU2* locus. To test functionality of the mutant proteins, 5-fold dilutions of cells suspended in YEP media were plated onto YEP plates containing 2% glucose (+D) or YEP containing 2% raffinose (+R) and 2% galactose (+G) and incubated at 25°C, 30°C, or 37°C for 2 days. To check expression of mutant Scc1 proteins, extracts from asynchronous cultures grown at 30°C in YEP+R+G were prepared by breaking cells in 10% CCl_3COOH and resuspension of the protein precipitate in SDS loading buffer. Scc1-HA_3 and its C-terminal cleavage product were detected after immunoblotting using 16B12 antibody (BAbCO). To test association of mutant Scc1 or Smc1 proteins, constructs were integrated at the *LEU2* locus of K7566 (*MATα, SMC1-myc$_{18}$::KITRP1*) or at the *URA3* locus of K7563 (*MATα, SCC1-HA$_6$::HIS3*), respectively. Extracts were prepared from asynchronous cultures grown at 30°C in YEP+D by breaking cells with glass beads in EBX buffer, and immunoprecipitations against the HA_3 (16B12) or myc_{18} (9E10) epitope tags were performed as described (Gruber et al., 2003).

Expression of Noncleavable Scc1 before and after Replication

Experiments were performed at 25°C. To arrest cells in metaphase by repressing the expression of Cdc20 from the *MET3* promoter, cells growing at logarithmic phase in −MET+R media were collected by filtration and resuspended in YEP+R media containing 2 mM methionine. After 1 hr, fresh methionine was added at 2 mM and cells were incubated for another 1.5 hr, after which more than 90% had arrested in metaphase. Scc1-HA_3 expression from the *GAL1-10* promoter was then induced for 3 hr by the addition of galactose to a final concentration of 2%. During this time, hourly samples were taken to analyze the protein levels of Scc1-HA_3 bound to chromatin by preparing extracts from spheroblasted cells and separating soluble extract from a chromatin-containing pellet as described (Liang and Stillman, 1997). Equal amounts of soluble and chromatin pellet fractions were probed for Scc1-HA_3 by immunoblotting (16B12). To induce Cdc20 expression from the *MET3* promoter and repress further Scc1-HA_3 expression from the *GAL1-10* promoter, cells were transferred into −MET+D media.

To arrest cells in G1 phase, α factor was added to 2 mg/l to cells growing at logarithmic phase in −MET+R media. After 1 hr, fresh α factor was added at 1.5 mg/l. After another 2 hr, more than 95% of the cells were arrested as small budded cells. Cells were collected by filtration and either directly transferred into YEP+R+G containing 2 mM methionine to release them from the arrest while inducing expression from the *GAL1-10* promoter, or cells were first transferred into YEP+R containing 2 mM methionine and galactose was added after 15, 30, 45, or 60 min. Samples were taken every 10 min after release to monitor the induced expression of Scc1-HA_3 and endogenous Scc1-myc_{18} on immunoblots. More than 95% of the cells had rearrested in metaphase 3 hr after release from α factor arrest. Cells were collected by filtration and released into −MET+D media.

Acknowledgments

We are grateful to Jan-Michael Peters, Vito Katis, Prakash Arumugam, and all lab members for advice and discussions. James Berger, Karl-Peter Hopfner, and Alexander Schleiffer communicated unpublished results. We thank all staff at ESRF beamline ID29, Grenoble, France. T.N. acknowledges support through a long-term EMBO fellowship. This work was supported by Boehringer Ingelheim International, the Austrian Industrial Research Promotion Fund (FFF), and the Austrian Science Fund (FWF).

Received: April 29, 2004
Revised: August 24, 2004
Accepted: August 24, 2004
Published: September 23, 2004

References

Anderson, D.E., Losada, A., Erickson, H.P., and Hirano, T. (2002). Condensin and cohesin display different arm conformations with characteristic hinge angles. J. Cell Biol. *156*, 419–424.

Arumugam, P., Gruber, S., Tanaka, K., Haering, C.H., Mechtler, K., and Nasmyth, K. (2003). ATP hydrolysis is required for cohesin's association with chromosomes. Curr. Biol. *13*, 1941–1953.

Chen, J., Lu, G., Lin, J., Davidson, A.L., and Quiocho, F.A. (2003). A tweezers-like motion of the ATP-binding cassette dimer in an ABC transport cycle. Mol. Cell *12*, 651–661.

Ciosk, R., Shirayama, M., Shevchenko, A., Tanaka, T., Toth, A., and Nasmyth, K. (2000). Cohesin's binding to chromosomes depends on a separate complex consisting of Scc2 and Scc4 proteins. Mol. Cell *5*, 243–254.

Gajiwala, K.S., and Burley, S.K. (2000). Winged helix proteins. Curr. Opin. Struct. Biol. *10*, 110–116.

Gruber, S., Haering, C.H., and Nasmyth, K. (2003). Chromosomal cohesin forms a ring. Cell *112*, 765–777.

Haering, C.H., Löwe, J., Hochwagen, A., and Nasmyth, K. (2002). Molecular architecture of SMC proteins and the yeast cohesin complex. Mol. Cell *9*, 773–788.

Hirano, M., Anderson, D.E., Erickson, H.P., and Hirano, T. (2001). Bimodal activation of SMC ATPase by intra- and inter-molecular interactions. EMBO J. *20*, 3238–3250.

Hopfner, K.P., Karcher, A., Shin, D.S., Craig, L., Arthur, L.M., Carney, J.P., and Tainer, J.A. (2000). Structural biology of Rad50 ATPase: ATP-driven conformational control in DNA double-strand break repair and the ABC-ATPase superfamily. Cell *101*, 789–800.

Lammens, A., Schele, A., and Hopfner, K.P. (2004). Structural biochemistry of ATP driven transport of DNA into SMC protein rings. Curr. Biol., in press.

Li, R., Manna, A.C., Dai, S., Cheung, A.L., and Zhang, G. (2003). Crystal structure of the SarS protein from Staphylococcus aureus. J. Bacteriol. *185*, 4219–4225.

Liang, C., and Stillman, B. (1997). Persistent initiation of DNA replication and chromatin-bound MCM proteins during the cell cycle in cdc6 mutants. Genes Dev. *11*, 3375–3386.

Locher, K.P., Lee, A.T., and Rees, D.C. (2002). The E. coli BtuCD structure: a framework for ABC transporter architecture and mechanism. Science *296*, 1091–1098.

Löwe, J., Cordell, S.C., and van den Ent, F. (2001). Crystal structure of the SMC head domain: an ABC ATPase with 900 residues antiparallel coiled-coil inserted. J. Mol. Biol. *306*, 25–35.

Melby, T.E., Ciampaglio, C.N., Briscoe, G., and Erickson, H.P. (1998). The symmetrical structure of structural maintenance of chromosomes (SMC) and MukB proteins: long, antiparallel coiled coils, folded at a flexible hinge. J. Cell Biol. *142*, 1595–1604.

Michaelis, C., Ciosk, R., and Nasmyth, K. (1997). Cohesins: chromosomal proteins that prevent premature separation of sister chromatids. Cell *91*, 35–45.

Moncalian, G., Lengsfeld, B., Bhaskara, V., Hopfner, K.P., Karcher, A., Alden, E., Tainer, J.A., and Paull, T.T. (2004). The rad50 signature motif: essential to ATP binding and biological function. J. Mol. Biol. *335*, 937–951.

Nikaido, K., Liu, P.Q., and Ames, G.F. (1997). Purification and characterization of HisP, the ATP-binding subunit of a traffic ATPase (ABC transporter), the histidine permease of Salmonella typhimurium. Solubility, dimerization, and ATPase activity. J. Biol. Chem. *272*, 27745–27752.

Schleiffer, A., Kaitna, S., Maurer-Stroh, S., Glotzer, M., Nasmyth, K., and Eisenhaber, F. (2003). Kleisins: a superfamily of bacterial and eukaryotic SMC protein partners. Mol. Cell *11*, 571–575.

Smith, P.C., Karpowich, N., Millen, L., Moody, J.E., Rosen, J., Thomas, P.J., and Hunt, J.F. (2002). ATP binding to the motor domain from an ABC transporter drives formation of a nucleotide sandwich dimer. Mol. Cell *10*, 139–149.

Stock, D., Perisic, O., and Löwe, J. (2004). Robotic nanolitre protein crystallisation at the MRC Laboratory of Molecular Biology. Prog. Biophys. Mol. Biol., in press.

Uhlmann, F., and Nasmyth, K. (1998). Cohesion between sister chromatids must be established during DNA replication. Curr. Biol. *8*, 1095–1101.

Uhlmann, F., Lottspeich, F., and Nasmyth, K. (1999). Sister-chromatid separation at anaphase onset is promoted by cleavage of the cohesin subunit Scc1. Nature *400*, 37–42.

Uhlmann, F., Wernic, D., Poupart, M.A., Koonin, E.V., and Nasmyth, K. (2000). Cleavage of cohesin by the CD clan protease separin triggers anaphase in yeast. Cell *103*, 375–386.

Weitzer, S., Lehane, C., and Uhlmann, F. (2003). A model for ATP hydrolysis-dependent binding of cohesin to DNA. Curr. Biol. *13*, 1930–1940.

Zubieta, C., He, X.Z., Dixon, R.A., and Noel, J.P. (2001). Structures of two natural product methyltransferases reveal the basis for substrate specificity in plant O-methyltransferases. Nat. Struct. Biol. *8*, 271–279.

Accession Numbers

Structure coordinates of the Smc1hd/Scc1-C dimer are available from the Protein Data Bank under accession number 1W1W.